Oriented Growth of ETS-4 Films Using the Method of Secondary Growth

Bilge Yilmaz, Kristin G. Shattuck, Juliusz Warzywoda, and Albert Sacco, Jr.*

Center for Advanced Microgravity Materials Processing, Department of Chemical Engineering, Northeastern University, 147 Snell Engineering Center, Boston, Massachusetts 02115

Received June 23, 2005. Revised Manuscript Received December 19, 2005

Oriented growth of polycrystalline ETS-4 films on porous titania substrates was investigated using the method of secondary growth, utilizing synthesis mixtures with compositions of $3.6SiO_2/1TiO_2/5.5Na_2O/xH_2SO_4/230.2H_2O$, where $x = 4.4$ or $x = 3.6$. Dense seed layers, obtained in situ by hydrothermal synthesis ($x = 4.4$), were partially (*a*, *c*)-out-of-plane oriented. Films were prepared in just one secondary growth step. Films developed by evolutionary, epitaxial growth of seed crystals and were highly ($x = 4.4$) *b*-out-of-plane oriented. Highly *b*-out-of-plane oriented ETS-4 films were also grown from dense, partially *b*-out-of-plane oriented seed layers on porous α-alumina substrates using identical synthesis mixtures. [Shattuck et al., *Microporous Mesoporous Mater.* **2006**, *88*, 56]. These findings suggest that the film orientation is dictated by the secondary growth conditions and is not determined by the seed layer orientation. This was attributed to the highly anisotropic growth rates of ETS-4 and the limited growth space provided by dense seed layers. Overall, these results indicate that by effectively decoupling nucleation from seed crystal growth, and by providing conditions for the fastest growth of crystals along the *b*-direction in a confined space, it is possible to fabricate highly *b*-out-of-plane oriented ETS-4 films for advanced applications.

1. Introduction

Nanowires with enhanced transport properties will constitute the heart of novel thermoelectric and photovoltaic devices.[2] Purely one-dimensional quantum transport characteristics can be realized for nanowires with diameters smaller than the de Broglie wavelengths (usually less than 10 nm). However, nanowires with dimensions on this scale cannot be obtained by using current conventional fabrication techniques. Titania is expected to be a superior semiconductor material for applications in photovoltaics; however, it is considered a challenge to grow titania in an anisotropic manner. Thus, it is currently not feasible to directly grow titania nanowires. Utilization of nanowires of various materials implanted in the pores of oriented films made of microporous or mesoporous molecular sieves was recently proposed.[2,3]

ETS-4 is a microporous titanosilicate molecular sieve with a framework structure composed of [SiO_4] tetrahedra, [TiO_5] semioctahedra, and [TiO_6] octahedra.[4,5] The [TiO_6] octahedra are linked to form linear monatomic ...Ti−O−Ti−O−Ti... chains, which are isolated from one another by a siliceous matrix made of [SiO_4] tetrahedra. As a result, these chains can behave as quantum wires.[6−8] Since the ...Ti−O−Ti−O−Ti... chains in ETS-4 crystals run in the [010] direction,[9] aligned crystals may provide oriented arrays of quantum wires. Thus, there is interest in growing *b*-out-of-plane oriented ETS-4 films (crystal *b*-directions preferentially oriented perpendicular to the substrate plane) in order to test the potential of ETS-4 crystals as quantum wire components of thermoelectric and photovoltaic devices. Supported ETS-4 films have also been proposed for conventional membrane applications such as gas separations, pervaporation, and fuel cells.[10] Fabrication of *b*-out-of-plane oriented ETS-4 films is desirable for these applications since the one-dimensional channel system that provides access to the interior of ETS-4 crystals runs in the *b*-direction.[10] Braunbarth et al.[10] obtained ETS-4 membranes on porous titania supports utilizing a multistep hydrothermal synthesis methodology. Seed layers, described as not preferentially oriented, were obtained in the first step using direct hydrothermal synthesis from gels performed during autoclave rotation. The secondary growth step was repeated up to five times to close the gaps between crystals in the film using clear solutions. This resulted in ETS-4 films with various degrees of *b*-out-of-plane orienta-

* Corresponding author. Phone: +1 617-373-7910. Fax: +1 617-373-8148. E-mail: asacco@coe.neu.edu.

(1) Shattuck, K. G.; Yilmaz, B.; Warzywoda, J.; Sacco, A., Jr. *Microporous Mesoporous Mater.*, **2006**, *88*, 56.
(2) Hillhouse, H. W.; Tuominen, M. T. *Microporous Mesoporous Mater.* **2001**, *47*, 39.
(3) Tsapatsis, M. *AIChE J.* **2002**, *48*, 654.
(4) Nair, S.; Jeong, H.-K.; Chandrasekaran, A.; Braunbarth, C. M.; Tsapatsis, M.; Kuznicki, S. M. *Chem. Mater.* **2001**, *13*, 4247.
(5) Kuznicki, S. M.; Bell, V. A.; Nair, S.; Hillhouse, H. W.; Jacubinas, R. M.; Braunbarth, C. M.; Toby, B. H.; Tsapatsis, M. *Nature* **2001**, *412*, 720.
(6) Yilmaz, B.; Miraglia, P. Q.; Warzywoda, J.; Sacco, A., Jr. *Microporous Mesoporous Mater.* **2004**, *71*, 167.
(7) Warzywoda, J.; Yilmaz, B.; Miraglia, P. Q.; Sacco, A., Jr. *Microporous Mesoporous Mater.* **2004**, *71*, 177.
(8) Yilmaz, B.; Warzywoda, J.; Sacco, A., Jr. *J. Cryst. Growth* **2004**, *271*, 325.
(9) Miraglia, P. Q.; Yilmaz, B.; Warzywoda, J.; Sacco, A., Jr. *J. Cryst. Growth* **2004**, *270*, 674.
(10) Braunbarth, C. M.; Boudreau, L. C.; Tsapatsis, M. *J. Membr. Sci.* **2000**, *174*, 31.

10.1021/cm051360u CCC: $33.50
Published on Web 02/01/2006

tion. Guan et al.[11] reported the fabrication of nonoriented ETS-4 membranes. In their procedure the outer surfaces of the tubular porous α-alumina supports were rubbed with ETS-4 powders for purposes of seeding. This was followed by the secondary growth of these seed crystals.[11] The authors did not provide details on the degree of coverage and adhesion of the seed layers on the support surface.

In the preparation of oriented zeolite/zeotype films by secondary growth of seed layers, secondary growth conditions must lead to (1) a slower nucleation rate compared with growth rates and (2) anisotropic growth rates of crystal faces with the fastest growth along the direction of desired film orientation.[12] Conventionally, clear/dilute solutions characterized by low supersaturation levels are used to better decouple nucleation from crystal growth. However, these solutions inherently decrease the rates of both processes. This may result in poorly intergrown/developed films (i.e., intercrystalline gaps in seed layers still exist after the secondary growth step). Thus, multiple secondary growth steps or longer processing times are used to improve the film continuity and/or orientation.[10,12]

Preparation of highly *b*-out-of-plane oriented ETS-4 films on porous α-alumina substrates from partially *b*-out-of-plane oriented seed layers was reported elsewhere.[1] This investigation identified the secondary growth conditions appropriate for the effective decoupling of nucleation from growth of seeds and the fastest growth of seed crystals along the *b*-direction. The objective of the present study was to examine the feasibility of hydrothermally growing highly *b*-out-of-plane oriented ETS-4 films from nonpreferentially (*b*-out-of-plane) oriented seed layers on porous titania substrates. Two gel compositions that provide a high driving force for both nucleation and crystal growth but result in different induction times of their respective ETS-4 crystallization curves[6] were utilized. The methodology used previously to grow oriented ETS-4 films on α-alumina substrates[1] was employed. The results of the present study are compared with those of Shattuck et al.[1] and discussed in terms of strategies that can be used to fabricate ETS-4 films with desirable *b*-out-of-plane orientation via oriented growth of seed layers.

2. Experimental Section

ETS-4 films were synthesized on porous titania (mean pore size ~0.1−0.2 μm, 35−40% void, Atraverda) substrates (~25 mm × ~5 mm × ~1 mm). A two-step synthesis procedure, which included direct in situ seed layer crystallization followed by secondary growth of seed crystals, was utilized. Prior to the synthesis procedure, substrates were cleaned by 10 min successive ultrasonication using a Branson 2200 ultrasonic cleaner in deionized water (resistivity >18 MΩ cm), methanol (99.5%, Aldrich), and 2-propanol (99.9%, Acros) followed by air-drying. In the seed layer formation step, substrates were diagonally placed in 10 mL Teflon-lined stainless steel autoclaves (Figure 1). Synthesis mixtures were then poured into the autoclaves. Syntheses were carried out for 24−72 h at 448 K under static conditions or under autoclave rotation at 72 rpm.

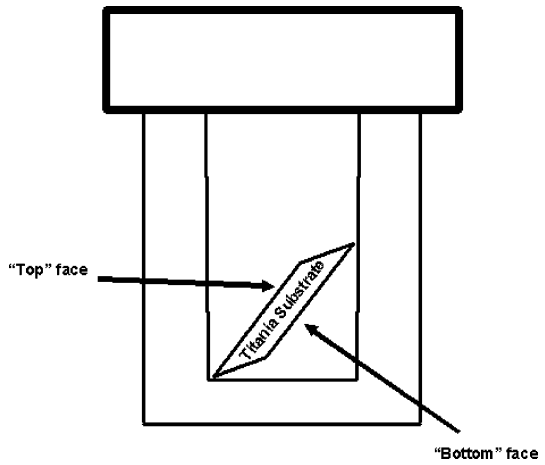

Figure 1. Schematic illustrating the orientation of the porous titania substrates in the autoclaves used in static hydrothermal synthesis of ETS-4 seed layers/films.

After the syntheses, the substrates were separated from the bulk products, washed with deionized water, and dried in ambient air for 2 h at 333 K. In the secondary growth step, substrates from the first step were again placed diagonally in the autoclaves (Figure 1), and synthesis mixtures were poured into the autoclaves. After static syntheses for 24−72 h at 448 K, the substrates were again separated from the bulk products, washed, and dried following the procedure described above. The bulk products from both steps were filtered, washed with deionized water, and dried overnight in ambient air at 333 K.

Synthesis mixtures with molar compositions of $3.6SiO_2/1TiO_2/5.5Na_2O/xH_2SO_4/230.2H_2O$ ($x = 3.6$ or $x = 4.4$) were prepared by combining two precursor solutions made in high-density polyethylene (HDPE) bottles. For the preparation of a typical synthesis mixture ($x = 4.4$), the titanium precursor solution was prepared by combining 5.547 g of TS-992 titanic sulfate (Kerr McGee Corp.), 0.707 g of sulfuric acid (96.5% H_2SO_4, Fisher), and 6.850 g of deionized water. The silicon precursor solution was obtained using 5.028 g of N-brand sodium silicate (PQ Corp.), 2.425 g of sodium hydroxide (97+% NaOH, Aldrich), and 14.443 g of deionized water. After combining these two precursor solutions, a white gel formed instantly. This gel was shaken vigorously by hand for ~2 min. The initial pH of synthesis mixtures was tested using an Orion pH meter model 720A (accuracy ±0.02).

Field emission scanning electron microscopy (FE-SEM) was used to image the morphology of bulk ETS-4 crystals, and coverage, size, morphology, intergrowth, and orientation of ETS-4 crystals in the seed layers/films, and to measure the seed layer/film thickness. The error in film thickness determination was ±0.5 μm. FE-SEM images of uncoated samples were obtained in the secondary electron imaging mode on a Hitachi S-4700 FE-SEM (10 μA emission current, 2 kV accelerating voltage, and 12 mm working distance). X-ray powder diffraction (XRD) was used for phase identification and to determine orientation of ETS-4 crystals in the seed layers/films. The XRD data were collected using Cu Kα radiation on a Bruker D5005 $\theta/2\theta$ Bragg−Brentano diffractometer (40 kV, 30 mA). The orientation of ETS-4 crystals in the seed layers/films was estimated by comparing the relative intensities of the ETS-4 peaks in the XRD patterns of the seed layers/films to those in the XRD pattern of ground bulk ETS-4 product obtained from static crystallization using the mixture with $x = 4.4$.

3. Results and Discussion

A representative top view FE-SEM image of the porous titania substrates is presented in Figure 2. As imaged, the

(11) Guan, G.; Kusakabe, K.; Morooka, S. *Microporous Mesoporous Mater.* **2001**, *50*, 109.
(12) Gouzinis, A.; Tsapatsis, M. *Chem. Mater.* **1998**, *10*, 2497.

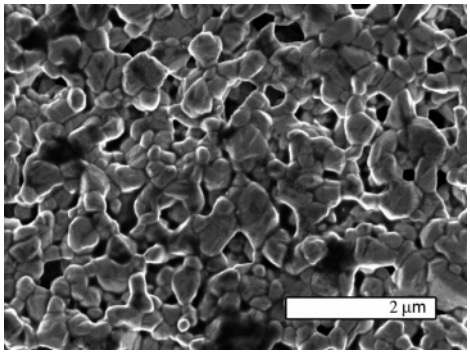

Figure 2. Top view FE-SEM image of the porous titania substrates.

substrate surface appeared similar to the titania supports used in previous studies.[10] A two-step procedure for controlling the orientation of ETS-4 films on these substrates was explored using synthesis mixtures with two compositions ($x = 4.4$ and $x = 3.6$). Direct in situ hydrothermal crystallization of seed layers was investigated under static conditions, as well as under autoclave rotation. Secondary growth of seed layers, which formed in the first step, was studied under static conditions only.

3.1. Seed Layer Formation. Static crystallization did not result in a successful seed layer formation for either composition (i.e., $x = 4.4$ or $x = 3.6$). However, bulk ETS-4 products were obtained, which were composed of particles with a cauliflower-like appearance. This is the typical morphology of spherulitic ETS-4 particles synthesized statically from mixtures with the same compositions, but in the absence of titania substrates.[6] Under autoclave rotation conditions, mixtures with $x = 3.6$ did not produce seed layers on titania substrates. Analogous results were obtained using α-alumina substrates in mixtures with the same composition.[1] This in part may be attributed to the partial dissolution of the substrate. Partial dissolution of α-alumina substrates upon hydrothermal treatment in these mixtures of relatively high alkalinity ($x = 3.6$, initial pH = 12.60) was observed before.[1] However, these observations may be also related to the chemistry of synthesis mixtures used in the seed layer formation step. In mixtures with $x = 4.4$, for example, the polycrystalline particles were composed of more crystallites, which were smaller (less than half the size) than those formed in mixtures with $x = 3.6$.[6]

Mixtures with lower alkalinity ($x = 4.4$, initial pH = 11.50) processed in rotating autoclaves produced seed layers on the titania substrates. These seed layers were composed of densely distributed, submicrometer-sized, intergrown crystals with platelike morphology (Figure 3). There were discernible gaps between platelets on the surface of seed layers (Figure 3a). The seed layers appeared to cover both sides (Figure 1) of the substrates equally (i.e., there was no significant variation of platelet dimensions, intergrowth, size distribution, surface coverage, and seed layer thickness as a function of the substrate side).

The (200) and (001) reflections of ETS-4 dominated the XRD patterns of these seed layers (Figure 4b) as seen by comparison to the XRD pattern of ground, bulk ETS-4 particles (Figure 4a). This indicates that the majority of ETS-4 crystals are oriented such that their *a*- or *c*-axes are

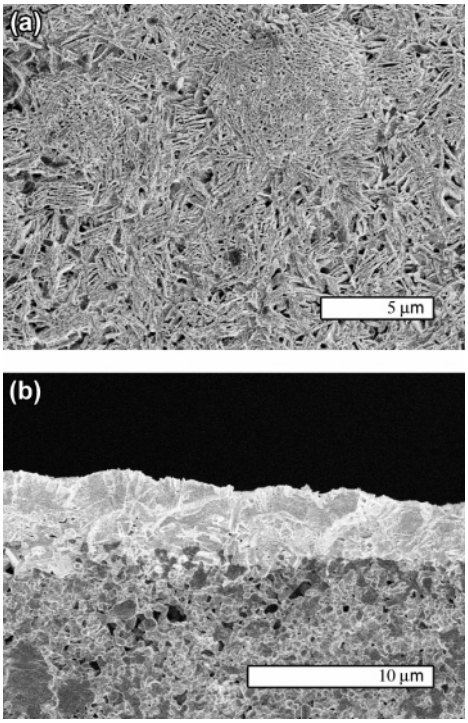

Figure 3. Typical top view (a) and cross-sectional (b) FE-SEM images of the ETS-4 seed layers obtained on porous titania substrates using mixtures with a molar composition of $3.6SiO_2/1TiO_2/5.5Na_2O/4.4H_2SO_4/230.2H_2O$ processed under autoclave rotation at 448 K.

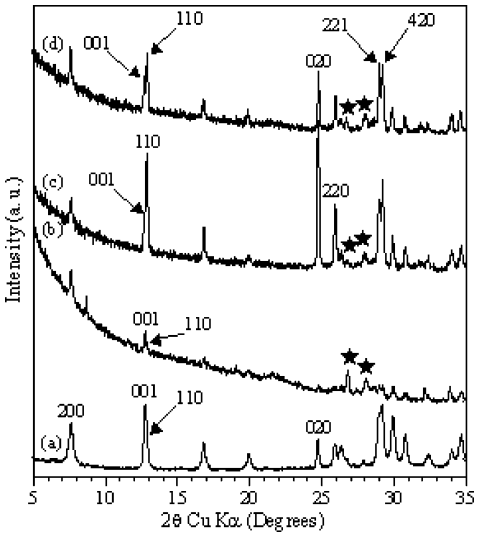

Figure 4. XRD patterns of ETS-4 grown at 448 K using mixtures with a composition of $3.6SiO_2/1TiO_2/5.5Na_2O/xH_2SO_4/230.2H_2O$: (a) ground bulk product obtained under static conditions, $x = 4.4$; (b) seed layer on a porous titania substrate obtained under autoclave rotation, $x = 4.4$; (c) film on the bottom face of a porous titania substrate obtained under static conditions, $x = 4.4$; (d) film on the bottom face of a porous titania substrate obtained under static conditions, $x = 3.6$. Star symbols depict the reflections due to the titania substrate.

perpendicular to the substrate plane. Consistent with this, a substantial decrease of the intensities of the (020) reflection and other reflections corresponding to crystallographic planes, whose directions are nearly parallel to the *b*-axis of ETS-4 crystals, was observed (Figure 4b). These seed layers can be described as partially (*a*, *c*)-out-of-plane oriented.

Although the seed layers on titania substrates were synthesized using the same synthesis mixture composition and processing conditions as those utilized in seed layer

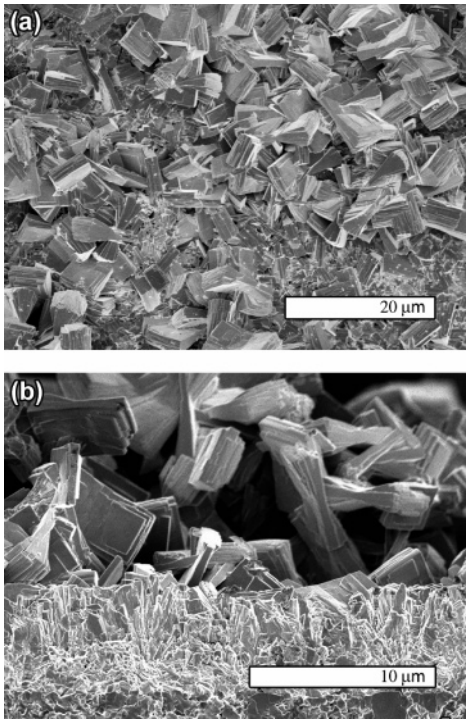

Figure 5. Typical top view (a) and cross-sectional (b) FE-SEM images of films grown at 448 K on the top faces of porous titania substrates using the statically processed mixtures with a molar composition of $3.6SiO_2/1TiO_2/5.5Na_2O/3.6H_2SO_4/230.2H_2O$.

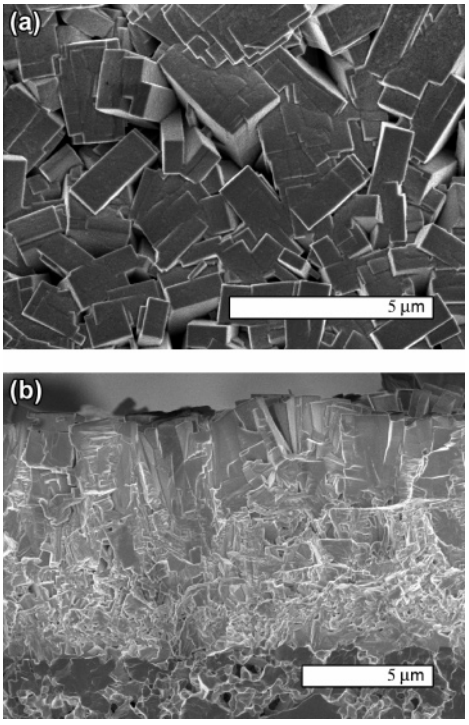

Figure 6. Typical top view (a) and cross-sectional (b) FE-SEM images of films grown at 448 K on the bottom faces of porous titania substrates using the statically processed mixtures with a molar composition of $3.6SiO_2/1TiO_2/5.5Na_2O/4.4H_2SO_4/230.2H_2O$.

formation on α-alumina substrates,[1] the microstructural characteristics of these seed layers were different. The platelets in the seed layers synthesized on the titania substrates appeared to be less uniformly distributed than platelets, which formed seed layers on α-alumina substrates. The linear dimensions of the platelets observed on the surfaces of seed layers on titania substrates were slightly larger on average and exhibited a greater variation compared to the linear dimensions of platelets forming surfaces of seed layers synthesized on α-alumina substrates. Finally, the seed layers obtained on titania substrates were partially (*a*, *c*)-out-of-plane oriented (vide supra), whereas seed layers synthesized on α-alumina substrates had partial *b*-out-of-plane orientation.[1] Differences in the surface characteristics (e.g., roughness, size, uniformity, and size distribution of pore mouths, etc.) of these two substrate types, and variation of the local synthesis mixture composition due to the possible titania substrate dissolution, likely contributed to the microstructural differences of the seed layers formed on the porous titania and α-alumina substrates. Different crystallographic texture (i.e., different crystal directions normal to the substrate) of the seed layers formed on each substrate type undoubtedly contributed to the differences in linear crystal dimensions and crystal size distributions observed on the surfaces of the respective seed layers.

3.2. Secondary Growth of Seed Layers. In the secondary growth step, which was performed using mixtures with both compositions ($x = 3.6$ or $x = 4.4$), the seed layer thickness increased from an initial value of ∼3.0−4.0 μm (Figure 3b) up to ∼10.0−11.0 μm (Figures 5−7). Bulk spherulitic particles formed in both cases (i.e., $x = 3.6$ and $x = 4.4$). Thus, the consumption of nutrients due to film growth was not sufficient to eliminate nucleation of new crystals. Films obtained on the top faces (Figure 1) of the substrates were covered by bulk ETS-4 particles either weakly (electrostatically) attached or randomly incorporated into the film (Figure 5). Films obtained on the bottom faces (Figure 1) of the substrates were devoid of such particles. Similar results were observed for α-alumina substrates.[1] Formations illustrated

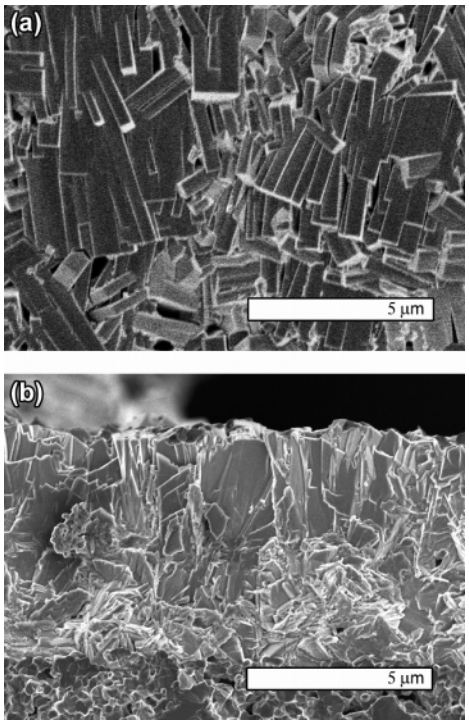

Figure 7. Typical top view (a) and cross-sectional (b) FE-SEM images of films grown at 448 K on the bottom faces of porous titania substrates using the statically processed mixtures with a molar composition of $3.6SiO_2/1TiO_2/5.5Na_2O/3.6H_2SO_4/230.2H_2O$.

in Figure 5 were likely due to settling/incorporation of new particles crystallized in the bulk solution in the later stages of the secondary growth step. Since the ETS-4 spherulite incorporation appeared to be limited to the topmost film surfaces only (Figures 5−7), the primary nucleation in the bulk solution did not contribute to the ETS-4 film growth. Thus, diagonal placement of the substrates in the autoclaves is a beneficial technique to preclude primary nucleation interference in the secondary growth of seed layers on the bottom faces (Figure 1) of the substrates.

The increased intensities of the (110), (020), (220), (221), and (420) reflections in the XRD patterns of ETS-4 films (Figure 4, parts c and d) compared to those characterizing ground bulk crystals (Figure 4a) indicated that substantially *b*-out-of-plane oriented films were obtained using mixtures with both compositions ($x = 4.4$ and $x = 3.6$). This is the desirable orientation for applications of ETS-4 films. On the basis of the more pronounced predominance of the (110), (020), and (220) reflections in their XRD patterns, films obtained using mixtures with $x = 4.4$ (Figure 4c) exhibited a higher degree of *b*-out-of-plane orientation than those grown using mixtures with $x = 3.6$ (Figure 4d). Similar results were obtained on α-alumina substrates using identical synthesis mixture compositions.[1] Since seed layers in each study differed in crystallographic texture (partial (*a*, *c*)-out-of-plane versus partial *b*-out-of-plane crystal orientation), the final film out-of-plane orientation is related more to the secondary growth conditions than to the initial crystal orientation distribution in seed layers.

Figures 6 and 7 show typical top view and cross-sectional images of ETS-4 films formed in the secondary growth step using mixtures with $x = 4.4$ and 3.6, respectively. In both cases, the predominant crystal dimensions observed on the film surface were at least 2 times larger than those observed on the surface of seed layers (Figures 3a, 6a, and 7a). More rigorous comparison of crystal dimensions cannot be performed since the crystallographic texture of seed layers and films is different (vide supra). The film thickness depended on the synthesis mixture used. The thickness of the film grown using synthesis mixture with $x = 4.4$ was ∼10.0−11.0 μm (Figure 6b), whereas the film thickness was ∼6.0−7.0 μm for the case of $x = 3.6$ (Figure 7b). This discrepancy in the thicknesses can be explained by the different timing of nucleation for these synthesis mixtures. A competition for nutrients is expected between the growing bulk crystals, which nucleated in the solution, and the crystals growing in the seed layer. ETS-4 synthesized from mixtures with $x = 3.6$ nucleates earlier in crystallization than ETS-4 grown from mixtures with $x = 4.4$.[6] Therefore, for synthesis mixtures with $x = 3.6$ bulk crystals would contribute more to the nutrient consumption, and thus, less nutrients would be available for growth of seed crystals, resulting in thinner films. This is what is observed.

Film cross sections revealed columnar grains (Figures 6b and 7b). No evidence of primary or secondary nucleation was observed throughout these columnar grains. This confirms that the experimental conditions were sufficient to effectively decouple nucleation from growth of the seed crystals. The in-plane crystal dimensions and degree of out-of-plane orientation in these films increased from those in seed layers (vide supra). These features indicate that these films developed predominantly by evolutionary selection due to the competitive growth of adjacent seed crystals according to the van der Drift growth model.[13−15] This implies that ETS-4 crystals at the surface of seed layers grew directly by epitaxy and that growth rates of crystal faces during the secondary growth step were anisotropic. In harmony with this finding, the order of the nonisometric growth velocities of ETS-4 crystal faces was previously reported as $V_{010} \gg V_{001} > V_{100}$.[9,16] In the secondary growth step, the few *b*-out-of-plane oriented seed crystals had the highest growth rate perpendicular to the substrate; hence, they grew fastest. As a result, they eventually outgrew their neighboring crystals. When a growing surface met the surface of its faster growing neighbor, an immobile grain boundary formed and the slower growth was annihilated. With time, as the film grew thicker, the fastest growing crystal orientation (*b*-out-of-plane) became increasingly dominant. Thus, development of the observed film texture was a natural consequence of this geometric selection process.

Highly oriented ETS-4 films with similar microstructural characteristics were observed to develop also on α-alumina substrates from dense, partially *b*-out-of-plane oriented seed layers, using identical synthesis mixtures.[1] Thus, in the observed self-orienting film growth, the direction of the emerging columnar microstructure did not depend on the initial seed crystal orientation. Evidently, the density and crystallographic orientation distribution of crystals in seed layers were sufficient to support highly oriented growth of films in a single secondary growth step. This can be attributed to the ETS-4 crystal growth anisotropy and competitive crystal growth in a confined growth space that caused the crystals growing in directions other than perpendicular (or nearly perpendicular) to the substrate surface to be quickly buried in the growth process. This further verifies that ETS-4 films evolved according to the van der Drift growth model. A higher degree of *b*-out-of-plane orientation of films grown using mixtures with $x = 4.4$ is consistent with their larger thickness since in the van der Drift model the texture distribution sharpens as the film thickens, with the maximum at an orientation that is determined by the fastest growing crystal direction.[14]

Overall, these findings demonstrated that the synthesis mixture with a higher driving force for nucleation ($x = 4.4$)[6] provided better secondary growth conditions (i.e., higher degree of *b*-out-of-plane film orientation) than the mixture with a lower nucleation rate ($x = 3.6$). Although this appears to be contrary to what can be expected as necessary for effective secondary growth, such an outcome can be inferred by examining crystallization curves for these two mixtures. The crystallization kinetics[6] for the mixture with $x = 4.4$ showed a longer induction time, which better decouples

(13) Xomeritakis, G.; Nair, S.; Tsapatsis, M. *Microporous Mesoporous Mater.* **2000**, *38*, 61.
(14) Smereka, P.; Li, X.; Russo, G.; Srolovitz, D. J. *Acta Mater.* **2005**, *53*, 1191.
(15) Thompson, C. V. *Annu. Rev. Mater. Sci.* **2000**, *30*, 159.
(16) Miraglia, P. Q.; Yilmaz, B.; Warzywoda, J.; Bazzana, S.; Sacco, A., Jr. *Microporous Mesoporous Mater.* **2004**, *69*, 71.

nucleation from crystal growth during that period, and a high crystallization rate, which provides a high driving force for growth. This is explained by the mechanism of spherulitic crystallization of ETS-4, where the higher viscosity[6] of the mixture with $x = 4.4$ limits the nucleation despite a considerable thermodynamic tendency for spontaneous three-dimensional nucleation. The anisotropic growth rates of ETS-4 crystals and the fastest growth along the *b*-direction are advantageous in preparation of *b*-out-of-plane oriented ETS-4 films. In conclusion, these observations suggest that utilization of synthesis mixtures with a long induction period in crystallization is an effective strategy to decouple nucleation from growth of seed crystals during film preparation via secondary growth of seed layers. Investigation of crystallization kinetics is essential when designing synthesis mixture compositions and processing conditions for film fabrication by the secondary growth method.

Unlike bulk ETS-4, which under static conditions grows by the low-angle branching mechanism,[6,8,9] ETS-4 crystals in seed layers appeared to grow predominantly by epitaxy. Verification of the contribution of the branching mechanism to the film formation may be difficult, since branching in ETS-4 occurs at small angles to the *b*-direction.[9] The apparently minimal contribution of the branching mechanism to the film development studied here may be due to the limited space available for branch development in the films synthesized. More exploration is needed to improve the understanding of the relative importance of low-angle branching in secondary growth of ETS-4 films.

4. Conclusions

Polycrystalline ETS-4 films were formed by secondary growth of seed layers obtained in situ by hydrothermal crystallization. Only one secondary growth step was employed to synthesize films. Highly *b*-out-of-plane oriented ETS-4 films were obtained. The film texture was not determined by the seed layer orientation. The anisotropy of ETS-4 growth was central in the development of the final film texture. This indicates that the density of seed layers was adequate to provide the confined growth space necessary for an effective self-alignment of crystals in one secondary growth step. No evidence of secondary nucleation was observed during film evolution. Thus, ETS-4 film growth followed the evolutionary selection principle of the van der Drift model of polycrystalline film growth. Synthesis mixtures with a high driving force for crystallization and a long induction period provided better secondary growth conditions. This is because the long induction period effectively decouples nucleation from crystal growth and the high crystallization rate provides a high driving force for growth. Analysis of the kinetics of crystallization prior to designing film growth conditions is essential in preparation of zeolite/zeotype films. The experimental conditions identified here, which provide self-orienting growth, can be used to fabricate *b*-out-of-plane oriented ETS-4 films desirable for both conventional and advanced applications.

Acknowledgment. The authors thank NASA for financial support.

CM051360U